Acid rain mediated nitrogen and sulfur deposition alters soil nitrogen, phosphorus and carbon fractions in a subtropical paddy

Chun Wang[a,b], Yunying Fang[c], Wanli An[a,b], Congsheng Zeng[a,b], Weiqi Wang[a,b,]*, Jordi Sardans[d,e,]*, Marcos Fernández-Martínez[d,e], Josep Peñuelas[d,e]

[a]*Institute of Geography, Fujian Normal University, Fuzhou 350007, China*

[b]*Key Laboratory of Humid Subtropical Eco-geographical Process, Ministry of Education, Fujian Normal University, Fuzhou 350007, China*

[c]*NSW Department of Primary Industries, Elizabeth Macarthur Agricultural Institute, Menangle, NSW 2568, Australia*

[d]*CSIC, Global Ecology Unit CREAF-CSIC-UAB, 08913 Bellaterra, Catalonia, Spain*

[e]*CREAF. 08913 Cerdanyola del Vallès, Catalonia, Spain*

*Corresponding authors at: Institute of Geography, Fujian Normal University, Fuzhou 350007, China.

E-mail addresses: wangweiqi15@163.com (W. Wang); j.sardans@creaf.uab.cat (J. Sardans)

ABSTRACT

Agricultural ecosystems are globally important sinks of carbon and other nutrient elements. In China, acid rain events affect about 0.62 million km^2, representing about 6.4% of total land area; however, the impacts of acid rain mediated nitrogen (N) and sulfur (S) depositions on soil carbon and nutrient stocks in paddy soils and implications for yield production under climate change are unclear. We conducted a field experiment during two annual crop seasons to determine the effects of simulated acid rain on soil organic carbon (SOC) fractions and nutrients in a subtropical paddy in China. Acid rain treatments comprised solutions of HNO_3 + H_2SO_4 to simulate N and S deposition at pH levels of 4.5, 3.5, and 2.5. The results showed that content of soil C fractions varied with acid rain pH. Acid rain led to increased SOC content and decreased ratios of soil labile organic carbon (LOC): SOC and dissolved organic carbon DOC: SOC concentration, independently of crop season and growth stage. Soil salinity was positively associated with SOC suggesting that higher levels of salinity inhibit C decomposition favoring SOC accumulation. Treatment effects of acid rain on soil microbial C and N depended on crop growth stage. Concentration of Fe^{2+} was positively correlated with DOC in early and late paddy soils under acid rain, possibly as a result of Fe^{2+} retention by DOC, when Fe^{3+} is reduced to Fe^{2+}. Acid rain led to increases in soil TN, TP, available N, NH_4^+ concentration, and SOC, and decreases in ratios of DOC: SOC, indicating decreases in soil biological activity and mineralization processes. Increases in dead rice plant biomass under acid rain were consistent with the increase in soil N and P concentrations, due to reduced nutrient uptake, and higher levels of total SOC.

Keywords: Organic carbon; Nutrient; Stoichiometry; Acid rain; Paddy

1. Introduction

Acid rain is a key environmental problem, because acidification influences soil nutrient storage and release processes (Rosi-Marshall et al., 2016), animal growth (Warren et al., 2017; Wei et al., 2017), plant growth (Medeiros et al., 2016), and soil metal leaching (Li et al., 2015). Acid rain has been shown to affect plant photosynthetic and antioxidant activities (Chen et al., 2013), physiological responses (Kováčik et al., 2011), and litter decomposition (Wang et al., 2012), and while a number of studies have investigated effects of simulated acid rain on soil respiration and its drivers in a subtropical mixed conifer and broadleaf forest (Liang et al., 2016), effects on organic carbon fractions remain unclear.

Global enhancement of carbon (C) sequestration in agricultural soils is considered a key measure to offset anthropogenic GHG emissions (Wang et al., 2015a, b), particularly in crops, such as rice paddy fields (Pan et al., 2004). Rice is a staple cereal crop for more than 50% of the global population (Haque et al., 2015); however, a 40% increase in its production by the end of 2030 is required to meet the food demands of the growing global population (FAO, 2009). Acid rain enhances photosynthetic parameters in rice, and hence grain yields (Wang et al., 2014a), and it general increases CO_2 emission and decreases the N nutrient availability (Ouyang et al., 2008), significant losses of major plant nutrients, such as potassium, calcium, and magnesium (Nawaz et al., 2012), increases recalcitrant organic matter (Wu et al., 2016). Rice cultivation plays an important role in the mitigation of atmospheric carbon dioxide (CO_2) (Lal, 2004), because the low soil organic C (SOC) content in paddy soils facilitates greater potential for sequestration of additional C under suitable management practices than soils with greater levels of SOC content (Pan et al., 2004; Wissing et al., 2011; Wang et al., 2015a), and it affects soil active C, which is the fraction of soil C with high levels of activity, due to impacts on plants and microorganisms and susceptibility to oxidation and decomposition (Kimura et al., 2004; Chen et al., 2010; Wang et al., 2015a). Nitrogen (N) inputs impact C and nutrient stoichiometry and, therefore, nutritional conditions required for microbe growth (Wang et al., 2014b), so the fraction of active C in paddy soil has been used as an indicator of management impacts on microbial and plant growth, and soil C dynamics (Purakayastha et al., 2008; Gong et al., 2009; Xu et al., 2011a,b).

Adequate levels of soil nutrients are essential to support the sustainable production of food (Ford et al., 2016); however, loss of nutrients creates environmental problems, such as eutrophication of water (Smith et al., 1999). Acid rain may affect soil nutrients directly through acidification and input of large amounts of active nutrients, such as N. Effects of acid rain may vary among nutrients, and with intensity and level of acidity; for example, soil NO_3^- and available P were reduced in tea plantation rhizosphere soil (Hu et al., 2017), while there was little effect on soil C and nutrient status (Chen et al., 2015). Effects of acid rain on soil nutrient status in paddy crops are unclear, although it is known that frequent periods of acid rain are associated with high levels of N and sulfur (S) deposition that indicate subsequent changes in soil chemistry, structure, C content, and nutrient status (Dise and Verry, 2001; Krusche et al., 2003; Hu et al., 2018).

Soil nutrient status drives ecosystem carbon sequestration and nutrient dynamics (Hessen et al., 2004), as a result of processes associated with litter C input (Wang et al., 2016), soil C concentration and storage (Wang et al., 2015c), and release of C from soils (Wang et al., 2014b). Besides nutrient stoichiometry, soil properties, such as iron dynamics (Peng et al., 2015), salinity (Wang et al., 2017a), water content (Wang et al., 2013), and pH (Jin and Wang, 2018) affect soil C fractions and nutrient content that are known to vary with rice growth (Wang et al., 2017b). However, effects of acid rain on variation in soil C fractions with rice crop growth stage are unclear.

China cultivates the second largest area of rice in the world, where 90% of the paddies are in the subtropics, such as in Fujian, Jiangxi, and Hunan Provinces. The development of strategies to increase the cost-effectiveness of rice agriculture and enhancement of crop yield and carbon sequestration from paddies has been investigated in subtropical China (Wang et al., 2015a, b). In China, acid rain affects an area of about 0.62 million km^2 (equivalent to about 6.4% of total land area), and this deposition is associated with inputs of N and S (about 24.2 and 21.1% of the total ion equivalent in acid rain, respectively) (Ministry of Ecology and Environment of the People's Republic of China, 2018) that is commonly occurring in several paddy areas of the country

(Larssen and Carmichael, 2000).

We aimed to determine the impacts of acid rain mediated N and S depositions on soil carbon and nutrient stocks in paddy soils and implications for yield production. We expected to provide a scientific basis for the effective assessment of the impact of acid rain on soil nutrient status and carbon sequestration. We also expected to provide suggestions for better responding to the impact of acid rain in future.

2. Materials and methods

2.1. Study site and experimental design

A field experiment was established in 2015 at the Fujian Academy of Agricultural Sciences, Fujian, southeastern China (119.3°E, 26.1°N,) (Fig. S1) during early (16 April to 16 July) and late (25 July to 6 November) paddy seasons. The proportions of sand, silt, and clay in the upper 15 cm of soil were 28, 60, and 12%, respectively, and other physicochemical properties comprised bulk density: 1.1 g cm^{-3}; pH: (1:5 with H_2O) 6.5; organic C content: 18.1 g kg^{-1}; total N content: 1.2 g kg^{-1}; and, total P content: 1.1 g kg^{-1} (Wang et al. 2014c, 2015b). Air temperature and humidity during the study period were shown in Fig. S2.

The paddy soils were plowed to a depth of 15 cm using a moldboard plow and then leveled immediately prior to transplantation of rice seedlings of 'Hesheng 10' and 'Qinxiangyou 212' in the early and late paddy seasons, respectively, using a rice transplanter, to a depth of 5 cm, and with plant and row spacings of 14 and 28 cm, respectively. Fertilizer was applied as NH_4-P_2O_5-K_2O (16-16-16; Keda Fertilizer Co., Ltd., Jingzhou, China) and urea (46% N), according to common agronomic practice in the region. Fertilizer was applied 1 d before transplantation (N, P, and K at 42, 40 and 40 kg ha^{-1}, respectively); during tiller-initiation, 7 d after transplantation (DAT), (N, P, and K at 35, 20, and 20 kg ha^{-1}, respectively); and, during panicle-initiation at 56 DAT; (N, P, and K at 18, 10, and 10 kg ha^{-1}, respectively). Paddy soils were flooded from 0 to 37 DAT, during which time, an automatic water-level controller was used to maintain water level at 5-7 cm above the soil surface. Then, the paddies were drained between 37 and 44 DAT; we maintained moist soils between 44 and 77 DAT for the early paddy and between 44 and 91 DAT for the late paddy. Paddies were drained 2 weeks before harvest (77 DAT for the early crop, 91 DAT for the late crop), and we harvested the rice crops at 92 DAT and 106 DAT for the early and late crops, respectively.

Three acid rain treatments, with pH 4.5, 3.5, and 2.5, were based on the acidity of rain water recorded in natural rain events in the study area (Table S1). Simulated acid rain was added every 7 d as simulated rainfall, as an amount equivalent to the local weekly mean rainfall during the respective paddy crop seasons, using mixed acid solutions of HNO_3 and H_2SO_4 (Wang et al., 2014a) to simulate N and S deposition. Three replicates of experimental and control plots were arranged in a randomized block design, where the 10-m^2 plots were separated by 0.5-cm thick, 30-cm high PVC plate (of which 20 cm was inserted into the soil) and a buffer zone of about 2 m. Control plots received non-acidified water. Plots were managed according to local common practice (Zhang et al., 2013; Wang et al., 2015a, b), and wooden bridges were constructed to minimize disturbance to soils during sample collection.

2.2. Determination of soil and rice properties

Soils were sampled (N = 72) during the rice greening, jointing, and mature stages (8, 78, and 92 DAT for the early paddy; 8, 64, and 106 for the late paddy) using a core sampler (0.3-m long, with 0.1-m diameter) from the upper 15-cm soil layer. The sample cores were divided into two parts, with one maintained at 4 °C for the measurement of soil microbial biomass carbon (MBC), microbial biomass nitrogen (MBN), available nitrogen (N), available phosphorus (P), and dissolved organic carbon (DOC), and the other was air-dried and finely ground using a ball mill, after all roots and visible plant remains had been removed, for determination of total soil organic carbon (SOC) and labile organic carbon (LOC).

DOC was determined by extracting C from the soils using 0.5 mol l^{-1} of K_2SO_4 and measuring its concentration using a TOC-V CPH total C analyzer (Shimadzu Scientific Instruments, Kyoto, Japan). MBC was determined using chloroform fumigation and extraction using 0.5 mol l^{-1} of K_2SO_4 (Lu, 1999) prior to measurement of C concentration using a TOC-V CPH total C analyzer (Shimadzu Scientific Instruments, Kyoto, Japan). MBN was determined using chloroform fumigation and extraction using 0.5 mol l^{-1} of K_2SO_4 (Lu, 1999) prior to measurement using a sequence flow analyzer (San^{++}, SKALAR Corporation production, Breda, The Netherlands); additional details are provided by Fang et al. (2018). Available P was extracted using the Mehlich method and measured using a sequence flow analyzer (San^{++}, SKALAR Corporation production, Breda, The Netherlands). Available N was calculated as the sum of NO_3^- and NH_4^+ in soil that was extracted using 2 mol l^{-1} of KCl and measured using a sequence flow analyzer (San^{++}, SKALAR Corporation production, Breda, The Netherlands). Total SOC and total N (TN) were determined using an Elementar Vario MAX CN Analyzer (Elementar Scientific Instruments, Hanau, Germany), and soil LOC was extracted using 333 mM of $KMnO_4$ in a digestion method (Xu et al., 2011b) and then determined using a UV-2450 spectrophotometer (Shimadzu Scientific Instruments, Kyoto, Japan). Soil total P (TP) concentration was measured extracted using perchloric-acid digestion and determined using a sequence flow analyzer (San^{++}, SKALAR Corporation production, Breda, The Netherlands).

Soil salinity and temperature were measured using a 2265FS EC/temperature meter (Spectrum Technologies Inc., Paxinos, USA), while soil pH (1:5 soil:water ratio) was measured using a Starter 300 pH meter (Ohaus Scientific Instruments, Parsippany, USA), and soil water content was measured using a TDR300 water content meter in situ (Spectrum Technologies Inc., Paxinos, USA). Total active Fe concentration was determined using a colorimetric method, where 1,10-phenanthroline was added to 1 mol l^{-1} HCl fresh-soil extracts to react with ferrous ions (Lu, 1999; Wang et al., 2014c). Ferric Fe concentration was calculated by subtracting concentration of ferrous Fe from that of total active Fe (Wang et al., 2014c). Rice height and grain yield were determined at the harvesting stage directly (Wang et al., 2014c).

2.3. Statistical analysis

We used general mixed models (GLM) in the "*nlme*" package in R, with the "*lme*" function (Pinheiro et al., 2016) to analyze the effects of acid rain independently of the season and growth stage, with acid rain season and growth stage as independent fixed categorical variables and plot as independent random factors with all soil studied variables as continuous dependent variables. Thereafter, we also analyzed the effects of acid rain within each crop season by similar mixed model but without season as fixed categorical independent variable.Non-normally distributed variables were log-transformed.. We chose the best model for each dependent variable based on the Akaike information criterion, and we used the MuMIn (Barton, 2012) R package to estimate the proportion of variance (%) explained by the mixed models. Tukey's post hoc tests (at $P < 0.05$) were used to detect treatment differences using the "*multcomp*" (Hothorn et al., 2013) R package, with the "*glht*" function.

Associations between soil organic fractions and properties were tested using Pearson correlation analysis and treatment effects were tested using Bonferroni's post hoc test (at $P < 0.05$). These analyses were performed using SPSS Statistics 18.0 (SPSS Inc., Chicago, USA).

Overall differences in soil traits among the four treatments were tested using a general discriminant analysis (GDA). Discriminant analyses consist of a supervised statistical algorithm that derives an optimal separation between groups established a priori by maximizing between-group variance, while minimizing within-group variance and controlling the effects of a categorical variable (here, season × crop stage) (Raamsdonk et al., 2001). Thus, GDA is a useful tool for the identification of variables that drive greatest differences among groups, and here, it allowed the discrimination of overall differences in soil traits under contrasting levels of acid rain independently of season and crop growth stage. Before conducting these multivariate analyses, we selected the sampling adequacy of individuals and the set of variables by the Barlett's test of sphericity (<0.05) and the Kaiser-Meyer-Olkin measure (>0.50). We removed the variables with communality values < 0.5 and perform GDA analyses with the variables with communality > 0.5. To perform these sampling adequacy analyses we used the package psych (Revelle, 2010). A cross-validation procedure (leave-one-out) was applied to test the adequacy of the discriminant model. GDAs were performed using Statistica 8.0 (StatSoft, Inc. Tulsa, USA).

3. Results

3.1. Effect of acid rain on soil carbon and nutrient concentrations and soil physyco-chemical variables.

Acid rain treatments led to greater levels of SOC, TN, soil N-avail, NO3-, TP and SWC, but lower pH, C:N, bacterial otus concentration, and ratios of LOC/SOC and DOC/SOC, regardless of crop season and crop growth stage (Table S2).

Analyzing the relationships of acid rain with the studied soil variables within each crop season, we observed between and within crop growth season some differences in several soil variables (Table S3, Fig. 1, Fig. S3). However, in both crop seasons, we observed that acid rain treatment decreased soil pH and increased TN, TP, SOC and N-availability (Table S3, Fig. 1-4). In early paddy season acid rain increased soil N-availability: P-availability ratio, soil water content and salinity and decreased soil C:N ratio (Table S3, Fig. 3 and 4). While in late paddy season acid rain was associated with an increase of soil NO_3^- and MBC concentrations and with lower LOC:SOC, DOC:SOC and MBC:SOC ratios and soil microbial otus concentrations (Table S3, Fig. 1-3). Soil TN and TP concentrations, and MBC:MBN ratios varied among rice growth stages (Table S3, Fig. 2,3). Ratios of soil C:P, N:P and LOC:available-N varied among rice growth stages in the two crop seasons (Table S3, Fig. 3).

Soil available N concentrations in early paddy soils were 45.5% greater in the pH 4.5 acid rain treatment than control. We found that soil NO_3^- concentrations were 81.7% greater in the pH 2.5 acid rain treatment than the control; however, NH_4^+ concentrations in early paddy soils were 49.4, 54.9, and 50.6% lower in the pH 4.5, 3.5, and 2.5 acid rain treatments, respectively, than the control. In early paddy soils, soil MBN was about 52.2 and 35.5% greater in the pH 4.5 and 2.5 acid rain treatments than the control, while in late paddy soils, it was about 27.4, 33.8, and 38.3% lower in the pH 4.5, 3.5, and 2.5 treatments, respectively, than the control. In early paddy soils, LOC:available N ratios were 22.5% lower in the pH 4.5 acid rain treatment than the control. Levels of soil Fe^{2+} concentration, salinity, and temperature varied among rice growth stages (Table S3, Fig. 5) in the two crop seasons, as did levels of soil water content and pH (Table S3, Fig. 4).

3.2. Physico-chemical soil variables (Fe, Salinity, SWC, temperature and pH.)

MBC was negatively correlated with DOC in early (r = -0.758, $P < 0.01$) and late (r = -0.436, $P < 0.01$) paddy soils (Table S4). Soil TN and NH_4^+ concentrations were positively correlated with DOC in early (r = 0.504 and 0.472, respectively, $P < 0.01$) and late (r = 0.341 and 0.749, respectively, $P < 0.05$) paddy soils, and soil available N was positively correlated with SOC and DOC in early (r = 0.503 and 0.654, respectively, $P < 0.01$) and late (r = 0.362 and 0.757, respectively, $P < 0.05$) paddy soils (Table 1). TP was positively associated with SOC in early (r = 0.811, $P < 0.01$) and late (r = 0.480, $P < 0.01$) paddy soils (Table 1). Ratio of LOC:available N was negatively correlated with SOC and DOC in early (r = -0.403 and -0.673, respectively, $P < 0.05$) and late (r = -0.333 and -0.579, respectively, $P < 0.05$) paddy soils, and the ratio of available N:available P was positively associated with DOC in early (r = 0.673, $P < 0.01$) and late (r = 0.631, $P < 0.01$) paddy soils (Table 1).

In general, soil salinity was positively correlated with SOC, and Fe^{2+} was positively correlated with DOC in the two crop seasons ($P < 0.05$, Table 1).

3.3. Effect of acid rain on rice yield and plant traits

There were no effects of acid rain treatment on rice yield or plant height in either crop season ($P > 0.05$). In early paddy soils, rice yields in the control and acid rain treatments pH 4.5, 3.5, and 2.5 were 4.63 ±0.52, 4.12 ±0.42, 4.37 ±0.11, and 4.55 ±0.42 Mg ha^{-1}, respectively, while in late paddy soils, they were 6.73 ±0.77, 5.89 ±0.25, 7.15 ±0.10, and 6.25 ±0.21 Mg ha^{-1}, respectively. Simulated acid rain resulted in greater proportions of moribund aboveground biomass at the end of the rice growth period, prior to harvest (data no shown).

3.4. Overall effects of simulated acid rain treatments on soil traits

GDA showed there were acid rain treatment effects on traits of paddy soils compared with untreated control soils, and between acid rain treatment pH 4.5 and the other two acid rain treatments (pH to 3.5 and 2.5); there were no overall differences in traits of soils treated with simulated acid rain at pH 2.5 and 3.5 (Tables 2, 3). The percent of correct predictions were 87.3%. Key drivers of differences in soil traits between the control and acid rain treatments along Root 1 were soil pH and SOC, where lower levels of higher pH and greater levels of SOC were associated with acid rain, while key drivers of differences between the pH 4.5 treatment and the pH 3.5 and 2.5 treatments along Root 2 were SOC, SWC, TP, DOC, Fe_3^{+}, and N_{avai}:P_{avai} ratio (Fig. 6).

4. Discussion

4.1. Effect of acid rain on carbon fractions, nutrient, and C, N, P stoichiometry

The results clearly showed that acid rain with N and S inputs as produced in natural events in China clearly increase SOC and soil total N and P. This is associated with a decrease of soil pH and more mortality in aboveground plant biomass. Thus, despite litter production increases following acid rain events, resulting in greater soil inputs of C, N, and P (Wang et al., 2012); the results strongly suggest that litter decomposition rates have decreased due to acid rain observing of LOC:SOC and LOC:SOC ratios and total soil P. This showed a lower rates of SOC conversion to DOC and LOC under acid rain consistent with the decrease of microbial community density.

Our finding that acid rain resulted in greater levels of soil TN and available N was consistent with the association between acid rain and N inputs (Rosi-Marshall et al., 2016) but also with the association of lower levels of pH and microbe inhibition (Babich and Stotzky, 1982). The very high rise in soil nitrate and a no clear rise in soil ammonium would be consistent with the rise of nitrification activity observed in other studies (Chao, 2010), and thus with higher mineralization of N and P and few N, P loss (Wang et al., 2012; Chen et al., 2015). The results also strongly suggest that the drop plant growth and nutrient uptake capacity (Malkanthi et al., 1995; Medeiros et al., 2016) linked to reduced root growth as observed in other studies (Liao and Chen, 1991; Kováčik et al., 2011; Medeiros et al., 2016) have conducted to an accumulation of C, N and P in soils. Thus, simulated acid rain at the level and characteristics as the observed in several cropland areas of China have a general short-time effect reducing soil pH and soil microbe content, associated to a rise in SOC and total N and P in soil associated all them to a drop in plant activity..

4.2. Effect of growth stage on soil properties, carbon fractions, nutrients, and C, N, and P stoichiometry

Concentrations of soil Fe^{2+}, water content, salinity, and temperature varied among rice growth stages in the two crop seasons. The greater levels of soil active Fe^{2+} concentrations at the greening growth stage than at the jointing and mature stages were related to greater anoxic soil conditions and, therefore, the reduction of Fe^{3+} to Fe^{2+} that occurred under flood conditions (Liu et al., 2013). However we have not observed changes in soil Fe2+ and Fe3+ concentrations the possible Fe^{3+} reduction by sulfate application, because sulfate-reduced products act as electron donors for the reduction of Fe^{3+} to Fe^{2+} (Nicol et al., 2016) as observed in other studies (Fry et al., 1986).

In general, we found that total SOC concentrations, soil TN, TP, available N, and available NH_4^+ concentrations varied among rice growth stages in the two crop seasons, coinciding with the rice crop phenology and with the periods of fertilizer application such as observed in previous studies (Bowatte et al., 2010; Wang et al., 2017b; Song et al., 2018; Wang et al., 2018a,b)..

4.3. Associations among soil carbon fractions, nutrients and stoichiometry, and soil traits

DOC was the active C resource for microbe growth; therefore, greater levels of DOC should have increased microbe growth (Schmidt et al., 1997; Wang et al., 2015a), however, we have observed that acid rain whereas increase DOC was associated to a decrease in soil microbe otus number. The decrease in microbes may reduce mineralization of SOC into labile carbon, such as DOC (Kunlanit et al., 2014), as reflected by decrease of microbe otus and the rise of DOC:SOC under acid rain.

Soil TN, available N, NH_4^+ concentration, and available N:available P ratios were positively associated with DOC in the two crop seasons, indicating the study paddy soils were N, rather than P-limited. This is consistent with the positive effects of N fertilization in the paddy soils of this cropland area (Zhang et al., 2009; Xu et al., 2010; Wang et al., 2014b; 2018c; Zhu et al., 2016). Overall, our data showed that acid rain decreased soil microbe biomass and SOC mineralization, despite greater availabilities of N and P that were probably related to decreased plant and microbial uptake. Thus, we suggest acid rain decreases biological activity, including mineralization of soil organic matter and plant-microbe uptake, that leads to increases in losses of available forms of nutrients and accumulation of C, N, and P soil recalcitrant fractions.

5. Conclusions

1. Acid rain increased SOC content and decreased ratios of soil LOC: SOC, DOC: SOC and MBC:SOC concentration ratios, whereas total soil N and P concentrations increased, indicating a decrease in soil mineralization and/or lower plant uptake.

2. Increased soil availability of N and P (P only in late paddy soils) under acid rain was likely related to diminished plant nutrient up-take, as supported by an increase in the proportion of dead rice plant biomass under acid rain.

3. The concentration of Fe^{2+} was positively correlated with DOC in early and late paddy soils under acid rain, possibly as a result of Fe^{2+} retention by DOC when Fe^{3+} is reduced to Fe^{2+}.

4. The observed increases in labile soil N and P, together with greater levels of SOC under acid rain strongly suggest that prolonged acid rain on paddy should favor the accumulation of C, N, and P recalcitrant fractions in soils leading to lower levels of soil fertility in paddy soils.

5. Soil TN, available N, NH_4^+ concentration, and ratio of available N:available P were positively associated with DOC in the two crop seasons, indicating the study site paddy soils were N, rather than P-limited. But the positive role on soil microbe and plant activity and SOC decomposition that can be expected from N deposition accompanying acid rain is counteracted by the negative effects of soil acidification.

Acknowledgments

The authors would like to thank Dengzhou Gao, Miaoying Wang, and Qiuli Zhu for assistance during field sampling. Funding was provided by the National Science Foundation of China (41571287, 31000209), Research Project of Public Institute of Fujian Province (2018R1034-1), Outstanding Young Research Talents in Higher Education of Fujian Province (2017), the European Research Council Synergy grant ERC-SyG-2013-610028 IMBALANCE-P, the Spanish Government grant PID2019-110521GB-I00, and the Catalan Government grant SGR 2017-1005.

Conflicts of Interest

The authors declare no conflicts of interest.

References

Babich, H., Stotzky, G., 1982. Nickel toxicity to microbes: effect of pH and implications for acid rain. Environ. Res. 29(2), 335–350.

Barton, K., 2012. MuM. In: Multi-model inference. R package version 1.7.2. http://CRAN. R-283 project.org/package=MuMIn. at http://cran.r-project.org/ package=MuMIn>.

Bowatte, S., Jia, Z., Ishihara, R., Nakajima, Y., Asakawa, S., Kimura, M., 2010. Molecular analysis of the ammonia oxidizing bacterial community in the surface soil layer of a japanese paddy field. Soil Sci. Plant Nutr. 52(4), 427–431.

Chao, W.L., 2010. Effects of acid rain on the nitrifying activity of copper amended soil. Lett. Appl. Microbiol. 21(1), 23–24.

Chen, H.L., Zhou, J.M., Xiao, B.H., 2010. Characterization of dissolved organic matter derived from rice straw at different stages of decay. J. Soil Sediment. 10, 915–922.

Chen, J., Wang, W.H., Liu, T.W., Wu, F.H., Zheng, H.L., 2013. Photosynthetic and antioxidant responses of *Liquidambar formosana* and *Schima superba* seedlings to sulfuric-rich and nitric-rich simulated acid rain. Plant Physiol. Bioch. 64, 41–51.

Chen, X., Chen, F., Ye, S., Yu, S., Fang, X., Hu, X., 2015. Responses of rhizosphere nitrogen and phosphorus transformations to different acid rain intensities in a hilly red soil tea plantation. Chin. J. Appl. Ecol. 26(1), 1–8.

Dise, N.B., Verry, E.S., 2001. Suppression of peatland methane emission by cumulative sulfate deposition in simulated acid rain. Biogeochemistry 53(2), 143–160.

Fang, Y., Singh, B.P., Luo, Y., Boersma, M., Zwieten, L.V., 2018. Biochar carbon dynamics in physically separated fractions and microbial use efficiency in contrasting soils under temperate pastures. Soil Biol. Biochem. 116, 399–409.

FAO [Food and Agricultural Organization of the United Nations]., 2009. OECD-FAO Agricultural Outlook 2011–2030.

Ford, H., Roberts, A., Jones, L., 2016. Nitrogen and phosphorus co-limitation and grazing moderate nitrogen impacts on plant growth and nutrient cycling in sand dune grassland. Sci. Total Environ. 542, 203–209.

Fry, I.V., Lazaroff, N., Packer, L., 1986. Sulfate-dependent iron oxidation by Thiobacillus ferrooxidans: characterization of a new EPR detectable electron transport component on the reducing side of rusticyanin. Arch. Biochem. Biophys. 246(2), 650–654.

Gong, W., Yan, X., Wang, J., Hu, T., Gong, Y., 2009. Long-term manuring and fertilization effects on soil organic carbon pools under a wheat-maize cropping system in North China Plain. Plant Soil 149, 318–324.

Haque, M.M., Kim, S.Y., Ali, M.A., Kim, P.J., 2015. Contribution of greenhouse gas emissions during cropping and fallow seasons on total global warming potential in mono-rice paddy soils. Plant Soil 387, 251–264.

Hessen, D.O., Ågren, G.I., Anderson, T.R., Elser, J.J., Ruiter, P.C.D., 2004. Carbon sequestration in ecosystems: the role of stoichiometry. Ecology 85(5), 1179–1192.

Hothorn, T., Bretz, F., Wesrfall, P., 2013. Package "*mulcomp*" (WWW document). U.R.L. http://cran.stat.sfu.ca/web/packages/mulcomp/mulcomp.pdf. (accessed 19.12.17).

Hu, M., Wilson, B.J., Sun, Z., Huang, J., Tong, C., 2018. Effects of nitrogen and sulphate addition on methane oxidation in the marsh soil of a typical subtropical estuary (min river) in China. Chem. Ecol. 34, 610–623.

Hu, X.F., Chen, F.S., Wine, M.L., Fang, X.M., 2017. Increasing acidity of rain in subtropical tea plantation alters aluminum and nutrient distributions at the root-soil interface and in plant tissues. Plant Soil 461, 261–274.

Jin, S., Wang, H., 2018. Relationships between soil pH and soil carbon in china's carbonate soils. Fresen. Environ. Bull. 27, 605–611.

Kimura, M., Murase, J., Lu, Y., 2004. Carbon cycling in rice field ecosystems in the context of input, decomposition and translocation of organic materials and the fates of their end products (CO_2 and CH_4). Soil Biol. Biochem. 36, 1399–1416.

.

Kováčik, J., Klejdus, B., Bačkor, M., Stork, F., Hedbavny, J., 2011. Physiological responses of root-less epiphytic plants to acid rain. Ecotoxicology 20(2), 348–357.

Krusche, A.V., de Camargo, P.B., Cerri, C.E., Ballester, M.V., Lara, L.B., Victoria, R.L., Martinelli, L.A., 2003. Acid rain and nitrogen deposition in a sub-tropical watershed (*piracicaba*): ecosystem consequences. Environ. Pollut. 121(3), 389–399.

Kunlanit, B., Vityakon, P., Puttaso, A., Cadisch, G., Rasche, F., 2014. Mechanisms controlling soil organic carbon composition pertaining to microbial decomposition of biochemically contrasting organic residues: evidence from middrifts peak area analysis. Soil Biol. Biochem. 76(1), 100–108.

Lal, R., 2004. Soil carbon sequestration impacts on global climate change and food security. Science 304,1623–1627.

Larssen, T., Carmichael, G.R., 2000. Acid rain and acidification in China: the importance of base cation deposition. Environ. Pollut. 110(1), 89–102.

Li, J., Jia, C., Lu, Y., Tang, S., Shim, H., 2015. Multivariate analysis of heavy metal leaching from urban soils following simulated acid rain. Microchem. J. 122, 89–95.

Liang, G., Hui, D., Wu, X., Wu, J., Liu, J., Zhou, G., Zhang, D., 2016. Effects of simulated acid rain on soil respiration and its components in a subtropical mixed conifer and broadleaf forest in southern China. Environ Sci.- Proc. Imp. 18(2), 246–255.

Liao, L., Chen, C., 1991. Effects of simulated acid rain on root growth of *Cunninghamia lanceolata* and *Schima superba* saplings planted in acidified soil. J. Environ. Sci. 3(2), 45–52.

Liu, Y., Li, F.B., Xia, W., Xu, J.M., Yu, X.S., 2013. Association between ferrous iron accumulation and pentachlorophenol degradation at the paddy soil-water interface in the presence of exogenous low-molecular-weight dissolved organic carbon. Chemosphere 91(11), 1547–1555.

Lu, R.K., 1999. Analysis methods of soil science and agricultural chemistry. Beijing: Agriculture Science and Technology Press.

Malkanthi, D.R.R., Yokoyama, K., Yoshida, T., Moritsugu, M., Matsushita, K., 1995. Effects of low pH and AI on growth and nutrient uptake of several plants. Soil Sci. Plant Nutr. 41, 161–165.

Medeiros, J.S., Tomeo, N.J., Hewins, C.R., Rosenthal, D.M., 2016. Fast-growing *Acer rubrum* differs from slow-growing *Quercus alba* in leaf, xylem and hydraulic trait coordination responses to simulated acid rain. Tree physiol. 36(8), 1032–1044.

Ministry of Ecology and Environment of the People's Republic of China., 2018. Bulletin on the state of China's ecological environment in 2017. pp 15–16.

Nawaz, R., Parkpian, P., Garivait, H., Anurakpongsatorn, P., Delaune, R.D., Jugsujinda, A., 2012. Impacts of acid rain on base cations, aluminum, and acidity development in highly weathered soils of Thailand. Commun. Soil Sci. Plan. 43(10), 1382–1400.

Nicol, M.J., Tjandrawan, V., Zhang, S., 2016. Cathodic reduction of iron(III) and copper(II) on various sulfide minerals in chloride solutions. Hydrometallurgy 166, 113–122.

Ouyang, X.J., Zhou, G.Y., Huang, Z.L., Liu, J.X., Zhang, D.Q., Jiong, L.I., 2008. Effect of simulated acid rain on potential carbon and nitrogen mineralization in forest soils. Pedosphere 18(4), 503–514.

Pan, G., Li, L., Wu, L., Zhang, X., 2004. Storage and sequestration potential of topsoil organic carbon in China's paddy soils. Global Change Biol. 10, 79–92.

Pinheiro, J., Bates, D., DebRoy, S., Sarkar, D., Core, T.R., 2016. *nlme*: Linear and Nonlinear Mixed Effects Models. R *package* version 3.1–126, http://CRAN.

Purakayastha, T.J., Rudrappa, L., Singh, D., Swarup, A., Bhadraray, S., 2008. Long-term impact of fertilizers on soil organic carbon pools and sequestration rates in maize-wheat-cowpea cropping system. Geoderma 144, 370–378.

Raamsdonk, L.M., Teusink, B., Broadhurst, D., Zhang, N.S., Hayes, A., Walsh, M.C., Berden, J.A., Brudle, K.M., Kell, D.K., Rowland, J.J., Westerhoff, H.V., van Dam, K., Oliver, S.G., 2001. A functional genomics strategy that uses metabolome data to reveal the phenotype of silent mutations. Nat. Biotechnol. 19, 45–50.

Revelle, W., 2010. Package “psych.” Retrieved August 24, 2010, from http://personality‐project.org/r/psych_manual.pdf

Rosi-Marshall, E.J., Bernhardt, E.S., Buso, D.C., Driscoll, C.T., Likens, G.E., 2016. Acid rain mitigation experiment shifts a forested watershed from a net sink to a net source of nitrogen. P. Natl. Acad. Sci. USA 113(27), 7580–7583.

Schmidt, I.K., Michelsen, A., Jonasson, S., 1997. Effects of labile soil carbon on nutrient partitioning between an arctic graminoid and microbes. Oecologia 112(4), 557–565.

Smith, V.H., Tilman, G.D., Nekola, J.C., 1999. Eutrophication: impacts of excess nutrient inputs on freshwater, marine, and terrestrial ecosystems. Environ. Pollut. 100(1–3), 179–196.

Song, Y., Song, C., Ren, J., Tan, W., Jin, S., Jiang, L., 2018. Influence of nitrogen additions on litter decomposition, nutrient dynamics, and enzymatic activity of two plant species in a peatland in northeast China. Sci. Total Environ. 625, 640–646.

Wang, C., Liu, X.T., Tong, C., Chen, X.X., Chen, Y.Y., Mou, X.J., Wan, S.A., 2017a. Effects of hydrologic and salinity gradients on soil organic carbon composition in Min river estuarine wetland. China Environ. Sci. 37(10), 3919–3928.

Wang, L., Wang, W., Zhou, Q., Huang, X., 2014a. Combined effects of lanthanum (III) chloride and acid rain on photosynthetic parameters in rice. Chemosphere 112, 355–361.

Wang, R.L., Christian, S., Dayan, F.E., Song, Y.Y., Su, Y.J., Zeng, R.S., 2012. Simulated acid rain accelerates litter decomposition and enhances the allelopathic potential of the invasive plant *wedelia trilobata* (creeping daisy). Weed Sci. 60(3), 462–467.

Wang, W., Lai, D.Y.F., Wang, C., Pan, T., Zeng, C., 2015a. Effects of rice straw incorporation on active soil organic carbon pools in a subtropical paddy field. Soil Till. Res. 152, 8–16.

Wang, W., Lai, D.Y.F., Abid, A.A., Neogi, S., Xu, X., Wang, C., 2018c. Effects of steel slag and biochar incorporation on active soil organic carbon pools in a subtropical paddy field. Agronomy 8, 135.

Wang, W., Lai, D.Y.F., Li, S., Kim, P.J., Zeng, C., Li, P., Liang, Y., 2014c. Steel slag amendment reduces methane emission and increases rice productivity in subtropical paddy fields in China. Wetl. Ecol. Manag. 22, 683–691.

Wang, W., Sardans, J., Lai, D.Y.F., Wang, C., Zeng, C., Tong, C., Liang, Y., Peñuelas, J., 2015b. Effects of steel slag application on greenhouse gas emissions and crop yield over multiple growing seasons in a subtropical paddy field in China. Field Crop. Res. 171, 146–156.

Wang, W., Sardans, J., Tong, C., Wang, C., Ouyang, L., Bartrons, M., Peñuelas, J., 2016. Typhoon enhancement of n and p release from litter and changes in the litter N:P ratio in a subtropical tidal wetland. Environ. Res. Lett. 11(1), 014003.

Wang, W., Sardans, J., Wang, C., Pan, T., Zeng, C., Lai, D., Bartrons, M., Peñuelas, J., 2017b. Straw application strategy to optimize nutrient release in a southeastern China rice cropland. Agronomy 7(4), 84.

Wang, W., Sardans, J., Wang, C., Zeng, C., Tong, C., Bartrons, M., Peñuelas, J., 2018b. Steel slag amendment increases nutrient availability and rice yield in a subtropical paddy field in China. Expl. Agric. 54, 842–856.

Wang, W., Sardans, J., Zeng, C., Zhong, C., Li, Y., Peñuelas, J., 2014b. Response of soil nutrient concentrations and stoichiometry to increased human disturbance in a subtropical tidal wetland. Geoderma 232–234, 459–470.

Wang, W., Wang, C., Sardans, J., Tong, C., Jia, R., Zeng, C., Peñuelas, J., 2015c. Flood regime affects soil stoichiometry and the distribution of the invasive plants in subtropical estuarine wetlands in China. Catena 128, 144–154.

Wang, W., Wang, C., Sardans, J., Tong, C., Ouyang, L., Asensio, D., Gargallo-Garriga, A., Peñuelas, J., 2018a. Storage and release of nutrients during litter decomposition for native and invasive species under different flooding intensities in a Chinese wetland. Aquat. Bot. 149, 5–16.

Wang, Y., Liu, X., Tang, C., Xu, J., 2013. pH change, carbon and nitrogen mineralization in paddy soils as affected by Chinese milk vetch addition and soil water regime. J. Soil Sediment. 13(4), 654–663.

Warren, D.R., Kraft, C., Josephson, D.C., Driscoll, C.T., 2017. Acid rain recovery may help to mitigate the impacts of climate change on thermally sensitive fish in lakes across eastern North America. Global Change Biol. 23(6), 2149–2153.

Wei, H., Liu, W., Zhang, J., Qin, Z., 2017. Effects of simulated acid rain on soil fauna community composition and their ecological niches. Environ. Pollut. 220, 460–468.

Wissing, L., Kölbl, A., Vogelsang, V., Fu, J., Cao, Z., Kögel-Knabner, I., 2011. Organic carbon accumulation in a 2000-year chronosequence of paddy soil evolution. Catena 87, 376–385.

Wu, J., Liang, G., Hui, D., Deng, Q., Xiong, X., Qiu, Q., Liu, J., Chu, G., Zhou, G., Zhang, D., 2016. Prolonged acid rain facilitates soil organic carbon accumulation in a mature forest in southern China. Sci. Total Environ. 544, 94–102.

Xu, M., Lou, Y., Sun, X., Wang, W., Baniyamuddin, M., Zhao, K., 2011b. Soil organic carbon active fractions as early indicators for total carbon change under straw incorporation. Biol. Fert. Soils 47, 745–752.

Xu, R., Wang, J., Zhang, G., Dai, Q., 2010. Changes of microbe and organic matter content in paddy soil applied with straw, manure and nitrogen fertilizer. Acta Ecol. Sin. 21(13), 3584–3590.

Xu, S., Shi, X., Zhao, Y., Yu, D., Li, C., Wang, S., Tan, M., Sun, W., 2011a. Carbon sequestration potential of recommended management practices for paddy soils of China, 1980–2050. Geoderma 166, 206–213.

Zhang, B., Pang, C., Qin, J., Liu, K., Xu, H., Li, H., 2013. Rice straw incorporation in winter with fertilizer-N application improves soil fertility and reduces global warming potential from a double rice paddy field. Biol. Fert. Soils 49, 1039–1052.

Zhang, L.M., Shan, L., Bouman, B.A.M., Xue, C.Y., Wei, F.T., Tao, H.B., Yang, X.G., Wang, H.Q., Zhao, D.L., Dittert, K., 2009. Response of aerobic rice growth and grain yield to n fertilizer at two contrasting sites near Beijing, China. Field Crop. Res. 114(1), 45–53.

Zhu, S., Vivanco, J.M., Manter, D.K., 2016. Nitrogen fertilizer rate affects root exudation, the rhizosphere microbiome and nitrogen-use-efficiency of maize. Appl. Soil Ecol. 107, 324–333.

Tables

Table 1

Pearson correlation analysis of association between carbon fractions and environmental factors.

Variable	Early paddy				Late paddy			
	SOC	DOC	MBC	EOC	SOC	DOC	MBC	LOC
TN	0.575**	0.504**	-0.535**	-0.031	0.253	0.341*	-0.078	-0.338*
Available N	0.503**	0.654**	-0.676**	0.058	0.362*	0.757**	-0.184	-0.217
NO_3^-	-0.301	0.384*	-0.200	-0.360*	0.213	-0.271	0.268	-0.062
NH_4^+	0.604**	0.472**	-0.568**	0.201	0.290	0.749**	-0.223	-0.187
Microbial N	-0.125	0.417*	-0.173	-0.259	-0.126	-0.158	0.423*	-0.044
TP	0.811**	-0.378*	0.256	0.175	0.480**	0.065	-0.225	-0.112
Available P	0.327	-0.106	-0.332*	0.362*	0.433**	0.202	0.132	0.187
C:N ratio	0.294	-0.742**	0.603**	0.305	0.361*	-0.164	0.081	0.283
C:P ratio	0.128	0.422*	-0.513**	0.134	0.380*	0.124	0.295	0.056
N:P ratio	-0.137	0.747**	-0.698**	-0.153	-0.086	0.182	0.102	-0.179
LOC:available N	-0.403*	-0.647**	0.627**	0.304	-0.333*	-0.579**	0.256	0.687**
LOC:available P	-0.094	0.019	0.191	0.445**	-0.261	-0.216	0.039	0.847**

available N:available P	0.397*	0.673**	-0.529**	-0.075	0.082	0.631**	-0.266	-0.310
MBC:MBN	0.283	-0.620**	0.618**	0.155	-0.012	-0.082	0.107	0.355*
Total Fe	-0.237	0.428**	-0.229	0.010	0.134	0.141	-0.177	0.113
Fe^{2+}	0.600**	0.441**	-0.527**	0.093	-0.015	0.533**	-0.325	-0.159
Fe^{3+}	-0.385*	0.320	-0.100	-0.012	0.167	-0.382*	0.130	0.291
Salinity	0.551**	0.159	-0.483**	0.399*	0.338*	0.690**	-0.210	-0.291
Water content	0.542**	0.309	-0.539**	0.372*	0.262	0.503**	-0.318	-0.022
pH	-0.044	0.275	-0.307	0.221	-0.373*	0.205	-0.099	0.056
Temperature	-0.244	-0.745**	0.745**	-0.084	0.232	0.626**	-0.231	-0.046

*$P < 0.05$; **$P < 0.01$.

621

Table 2

Discriminant analysis of treatment effects on soil traits (independent continuous variables), with season as a categorical independent factor.

	pH 4.5	pH 3.5	pH 2.5
Control	M = 49.9 F = 8.76 $P < 0.00001$	M =5 5.4 F = 9.72 $P < 0.00001$	M = 10.5 F = 10.0 $P < 0.00001$
pH 4.5		M = 7.61 F = 1.38 $P = 0.17$	M = 14.4 F = 2.52 $P = 0.004$
pH 3.5			M = 11.8 F = 2.03 $P = 0.019$

Table 3

General discriminant analysis (Wilks' λ and *P*) of soil variables。

Test	Value	*F*	*P*
pH	0.602	8.80	<0.0001
Fe^{2+}	0.758	4.25	0.011
Fe^{3+}	0.823	2.86	0.049
salinity	0.828	2.78	0.049
Water %	0.713	5.378	0.0033
temperature	0.974	0.368	0.78
SOC	0.630	7.828	0.0003
DOC	0.881	1.80	0.16
MBC	0.939	0.871	0.46
LOC/SOC	0.886	1.72	0.18
DOC/SOC	0.874	1.93	0.14
MBC/SOC	0.944	0.794477	0.50
NO_3^-	0.972	0.381	0.77
NH_4^+	0.948	0.730	0.54
MBN	0.859	2.19	0.10
Total P	0.871	1.98	0.13
Available P	0.827	2.79	0.053
C/N	0.866	2.07	0.12
C/P	0.871	1.98	0.13
N/P	0.904	1.42	0.25
LOC/N-available	0.840	2.53	0.070
LOC/P-available	0.847	2.43	0.081
N-available/P-available	0.950	0.706	0.55
MBC/MBN	0.858	2.20	0.10
timing	0.596	1.52	0.11

Figure legends

Fig. 1. Treatment effects on SOC, LOC, DOC, and MBC in early (A, C, E, and G, respectively) and late (B, D, F, and H, respectively) paddies. Data are means ±SE. Different uppercase letters indicate treatment differences among rice growth stages and lowercase letters indicate treatment differences within a rice growth stage ($P < 0.05$).

Fig. 2. Treatment effects on total N, available N, NO_3^-, NH_4^+, MBN, total P, and available P in early (A, C, E, G, I, K, and M, respectively) and late (B, D, F, H, J, L, and N, respectively) paddies. Data are means ±SE. Different uppercase letters indicate treatment differences among rice growth stages and lowercase letters indicate treatment differences within a rice growth stage ($P < 0.05$).

Fig. 3. Treatment effects on ratios of C:N, C:P, N:P, LOC:available N, LOC:available P, available N:available P, and MBC:MBN in early (A, C, E, G, I, K, and M, respectively) and late (B, D, F, H, J, L, and N, respectively) paddies. Data are means ±SE. Different uppercase letters indicate treatment differences among rice growth stages, and lowercase letters indicate treatment differences within a rice growth stage ($P < 0.05$).

Fig. 4. Treatment effects on salinity, water content, temperature, and pH in early (A, C, E, and G, respectively) and late (B, D, F, and H, respectively) paddies. Data are means ±SE. Different uppercase letters indicate treatment differences among rice growth stages and lowercase letters indicate treatment differences within a rice growth stage ($P < 0.05$).

Fig. 5. Treatment effects on total active Fe, Fe^{2+}, and Fe^{3+} in early (A, C, and E, respectively) and late (B, D, and F, respectively) paddies. Data are means ±SE. Different

uppercase letters indicate treatment differences among rice growth stages and lowercase letters indicate treatment differences within a rice growth stage ($P < 0.05$).

Fig. 6. GDA biplot of treatment effects on soil traits by grouping factor (treatment by season). Data are means ±95% CI and the standardized canonical discriminate function coefficients for the first two roots represent the soil variables as independent variables. pH: soil pH; Fe^{2+}: soil Fe^{2+} concentration; Fe^{3+}: soil Fe^{2+} concentration; salinity: soil salinity; SWC: soil water content; T: soil temperature; DOC: dissolved organic carbon; SOC: soil organic carbon; MBC: microbial carbon concentration; MBN: microbial nitrogen concentration; NO_3^-: soil nitrate ion concentration; NH_4^+: soil ammonium concentration; TP: soil total P concentration; avaiP: soil P plant availability; C:N: soil total C:N ratio; C:P: soil total C:P ratio; N:P: soil total N:P ratio; MBC:MBN: MBC:MBN ratio; LOC:Navai: LOC:available N ratio; LOC:Pavai: LOC:available P ratio; DOC:SOC: DOC:SOC ratio; MBC:SOC: MBC:SOC ratio; Navai:Pavai: Navai:Pavai ratio; and, LOC:SOC: LOC:SOC ratio.

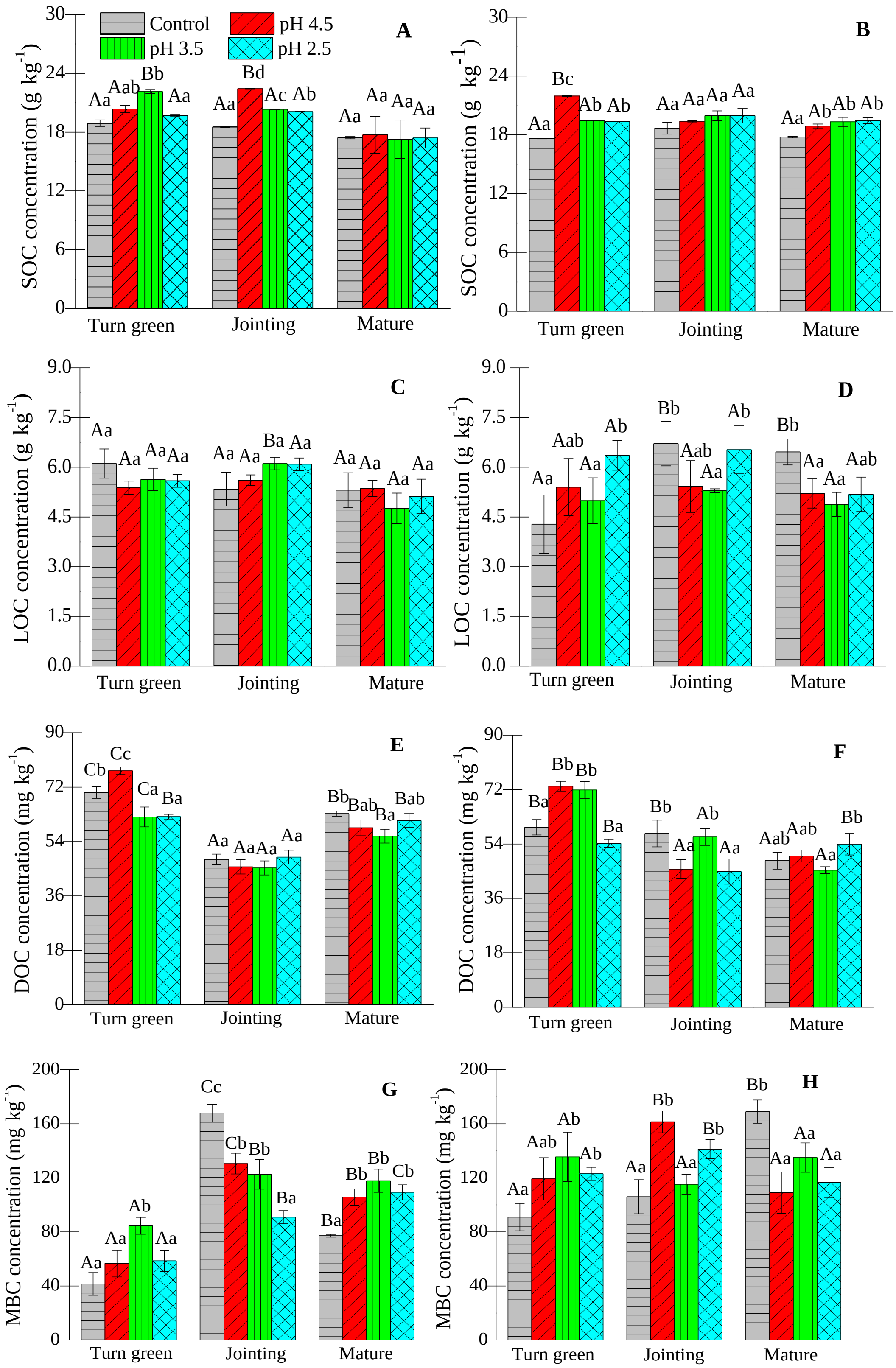
Control
pH 4.5
pH 3.5
pH 2.5
A
B
C
D
E
F
G
H
SOC concentration (g kg-1)
LOC concentration (g kg-1)
DOC concentration (mg kg-1)
MBC concentration (mg kg-1)
Turn green
Jointing
Mature

Fig. 1.

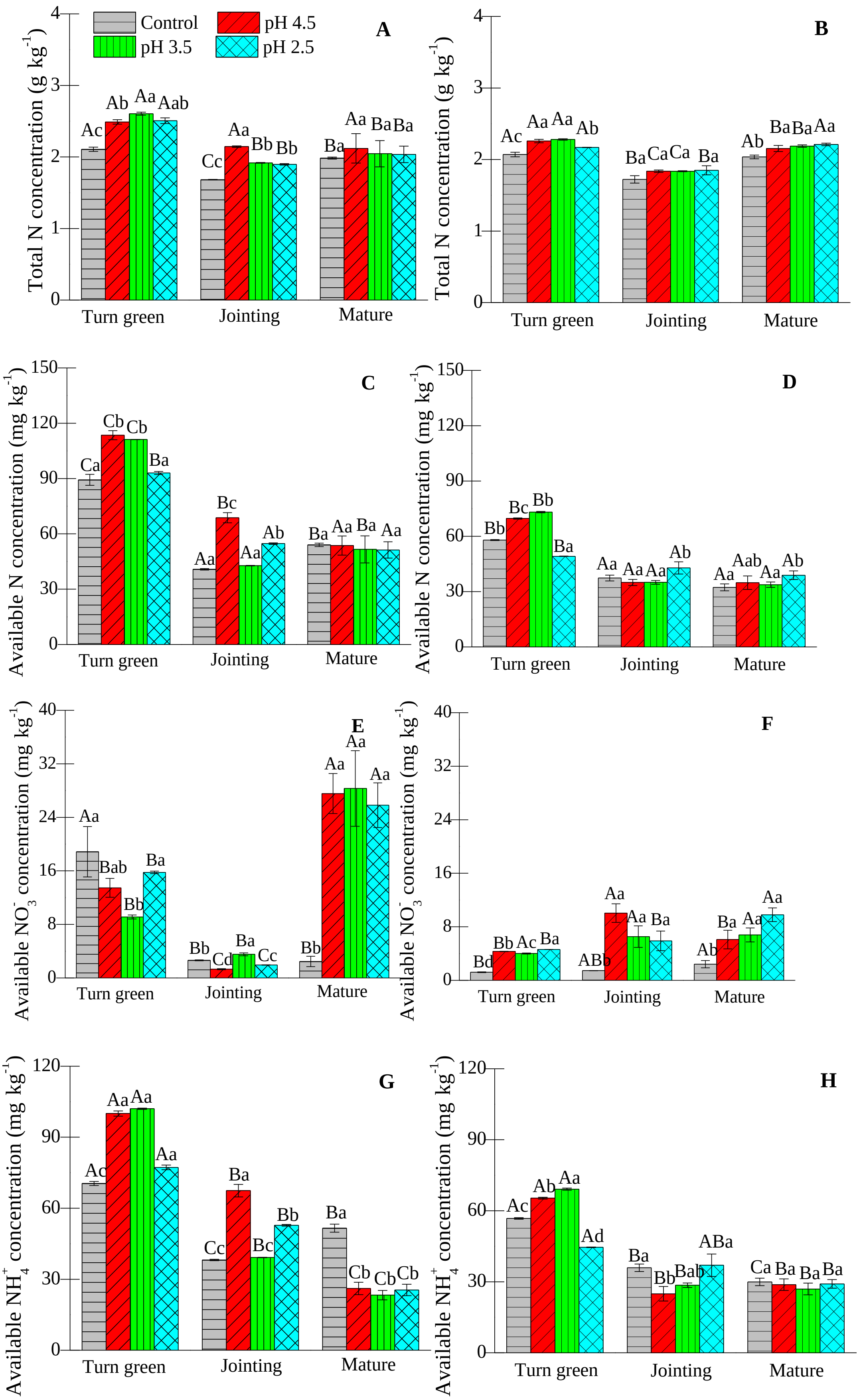
A
B
C
D
E
F
G
H
Control
pH 4.5
pH 3.5
pH 2.5
Total N concentration (g kg-1)
Available N concentration (mg kg-1)
Available NO3- concentration (mg kg-1)
Available NH4+ concentration (mg kg-1)
Turn green
Jointing
Mature
Ac Ab Aa Aab
Cc Aa Bb Bb
Ba Aa Ba Ba
Ac Aa Aa Ab
Ba Ca Ca Ba
Ab Ba Ba Aa
Ca Cb Cb Ba
Aa Bc Aa Ab
Ba Aa Ba Aa
Bb Bc Bb Ba
Aa Aa Aa Ab
Aa Aab Aa Ab
Aa Bab Bb Ba
Bb Cd Ba Cc
Bb Aa Aa Aa
Bd Bb Ac Ba
ABb Aa Aa Ba
Ab Ba Aa Aa
Ac Aa Aa Aa
Cc Ba Bc Bb
Ba Cb Cb Cb
Ac Ab Aa Ad
Ba Bb Bab ABa
Ca Ba Ba Ba

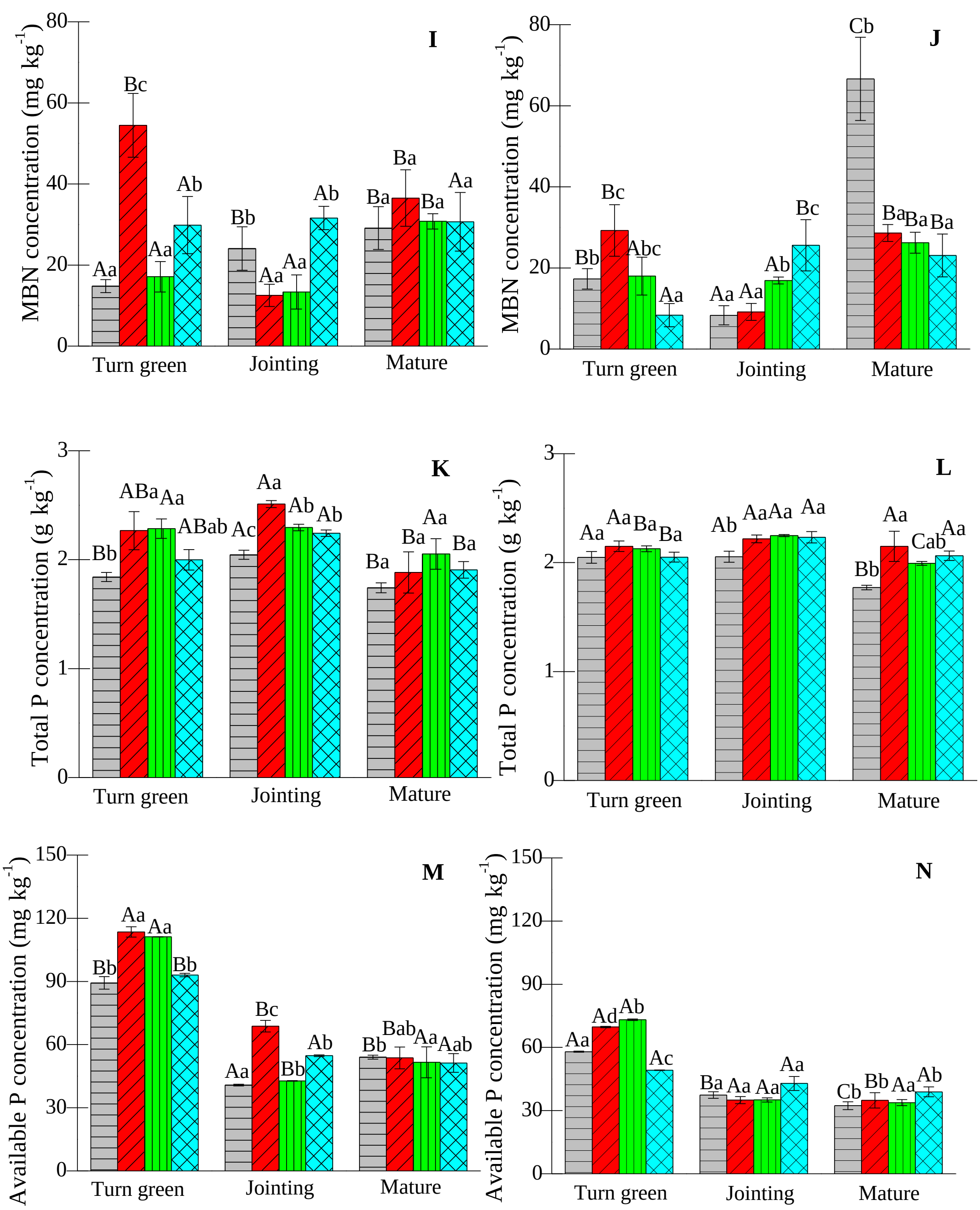
I
J
K
L
M
N
MBN concentration (mg kg-1)
Total P concentration (g kg-1)
Available P concentration (mg kg-1)
Turn green
Jointing
Mature

Fig. 2.

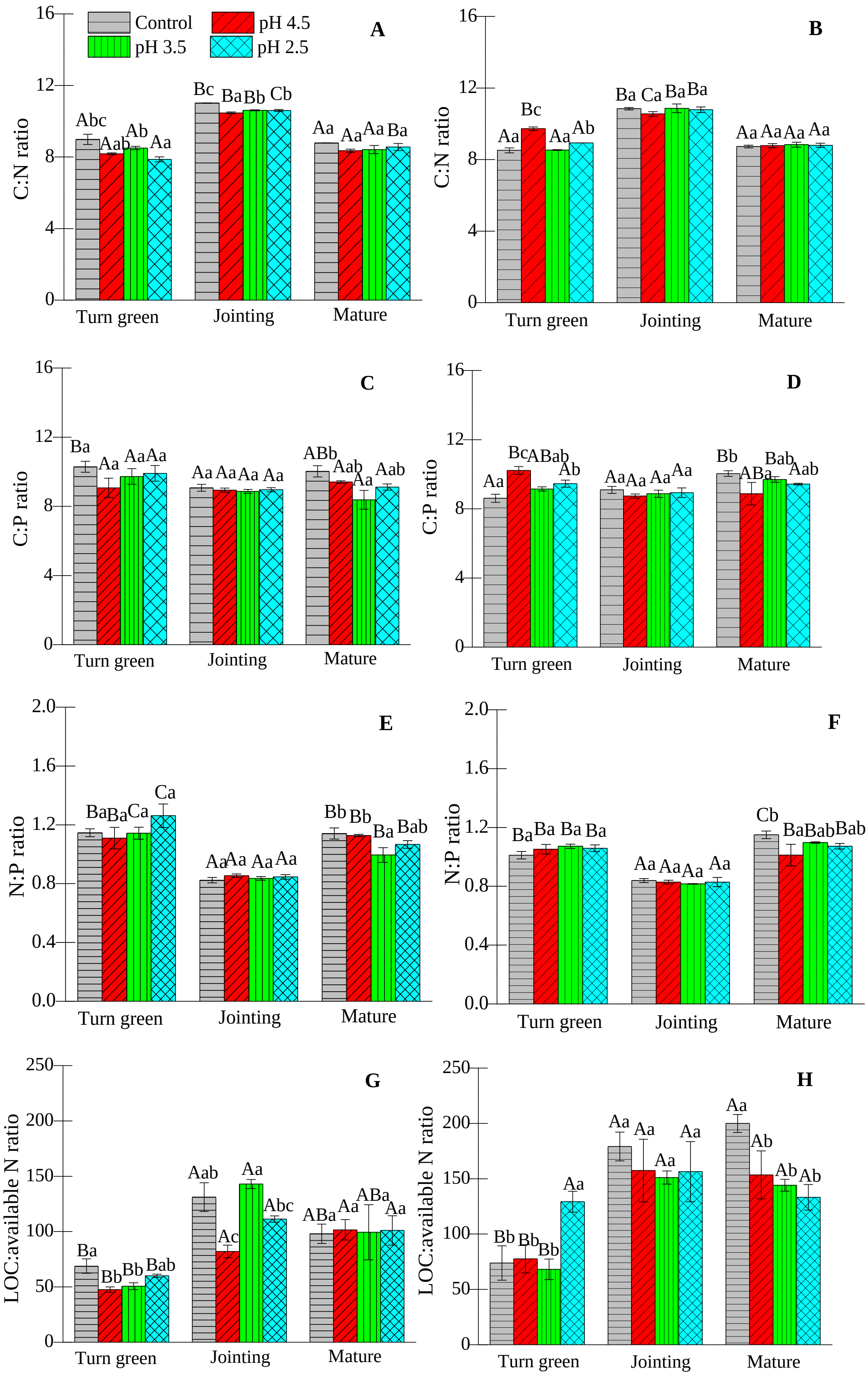
Control
pH 4.5
pH 3.5
pH 2.5
A
B
C
D
E
F
G
H
C:N ratio
C:P ratio
N:P ratio
LOC:available N ratio
Turn green
Jointing
Mature

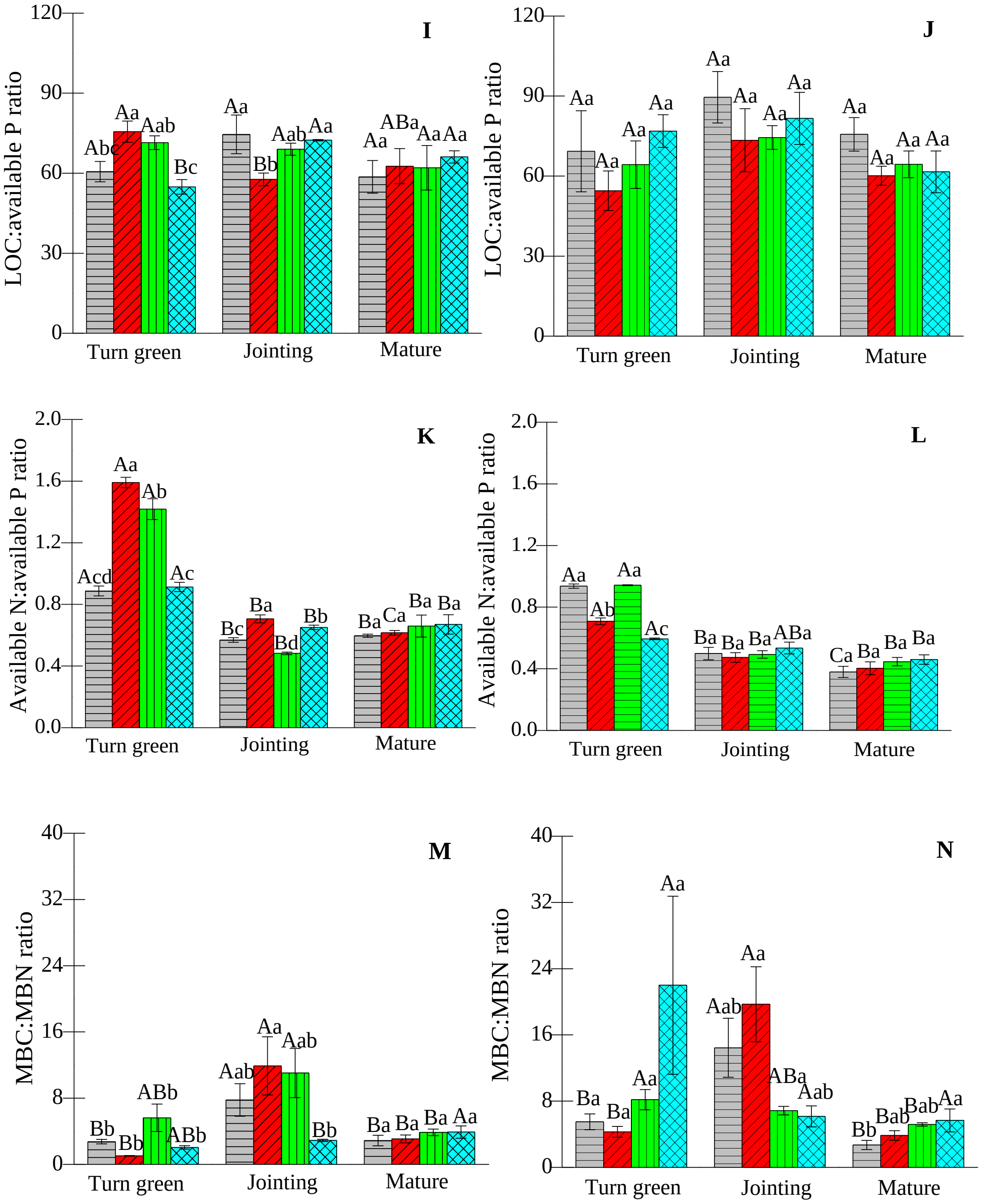
I
LOC:available P ratio
120
90
60
30
0
Abc Aa Aab Bc
Aa Bb Aab Aa
Aa ABa Aa Aa
Turn green
Jointing
Mature
J
LOC:available P ratio
120
90
60
30
0
Aa Aa Aa Aa
Aa Aa Aa Aa
Aa Aa Aa Aa
Turn green
Jointing
Mature
K
Available N:available P ratio
2.0
1.6
1.2
0.8
0.4
0.0
Acd Aa Ab Ac
Bc Ba Bd Bb
Ba Ca Ba Ba
Turn green
Jointing
Mature
L
Available N:available P ratio
2.0
1.6
1.2
0.8
0.4
0.0
Aa Ab Aa Ac
Ba Ba Ba ABa
Ca Ba Ba Ba
Turn green
Jointing
Mature
M
MBC:MBN ratio
40
32
24
16
8
0
Bb Bb ABb ABb
Aab Aa Aab Bb
Ba Ba Ba Aa
Turn green
Jointing
Mature
N
MBC:MBN ratio
40
32
24
16
8
0
Ba Ba Aa Aa
Aab Aa ABa Aab
Bb Bab Bab Aa
Turn green
Jointing
Mature

Fig. 3.

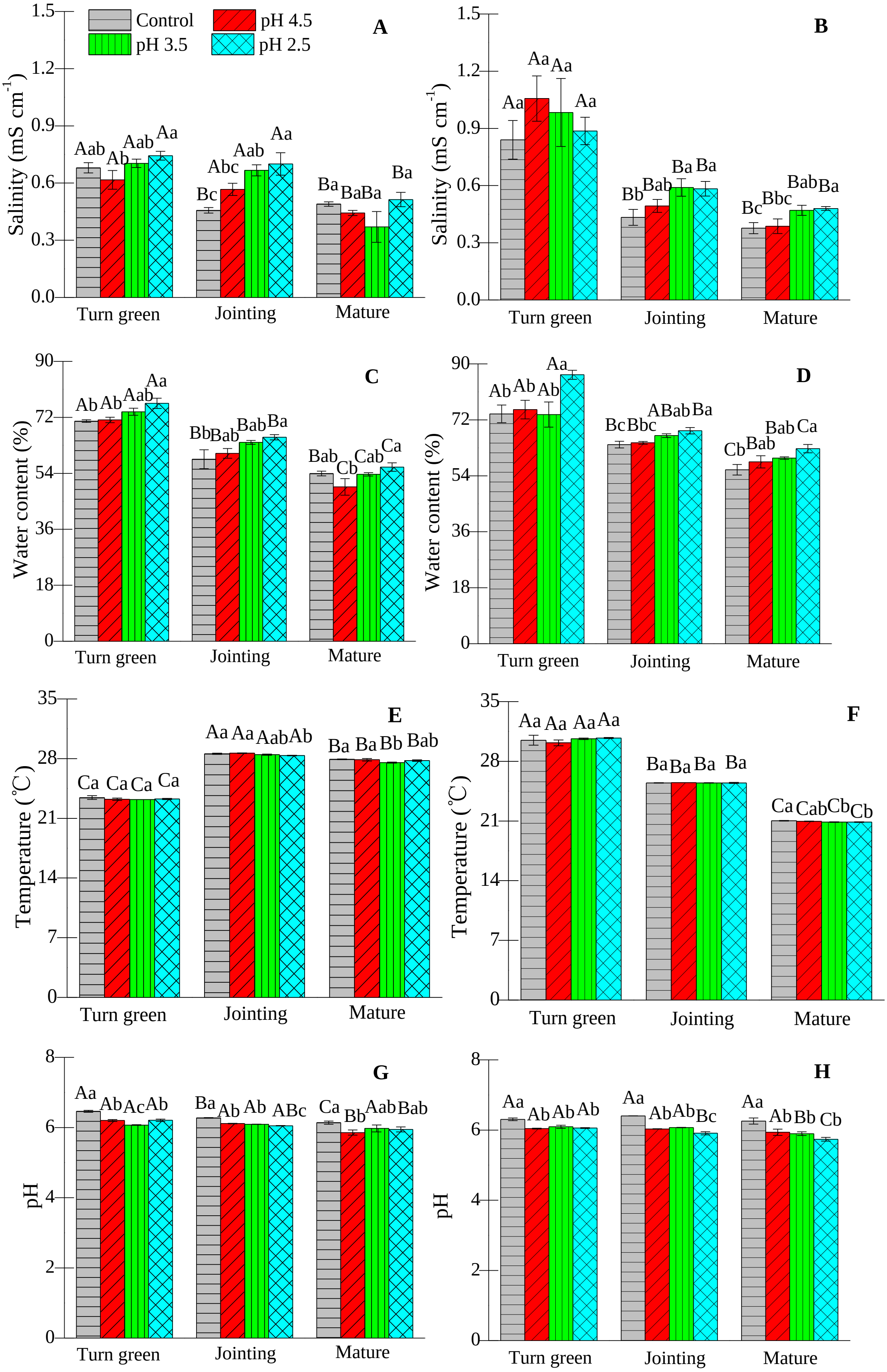
Control
pH 4.5
pH 3.5
pH 2.5
A
B
C
D
E
F
G
H
Salinity (mS cm-1)
Water content (%)
Temperature (°C)
pH
1.5
1.2
0.9
0.6
0.3
0.0
90
72
54
36
18
0
35
28
21
14
7
8
6
4
2
Turn green
Jointing
Mature

Fig. 4.

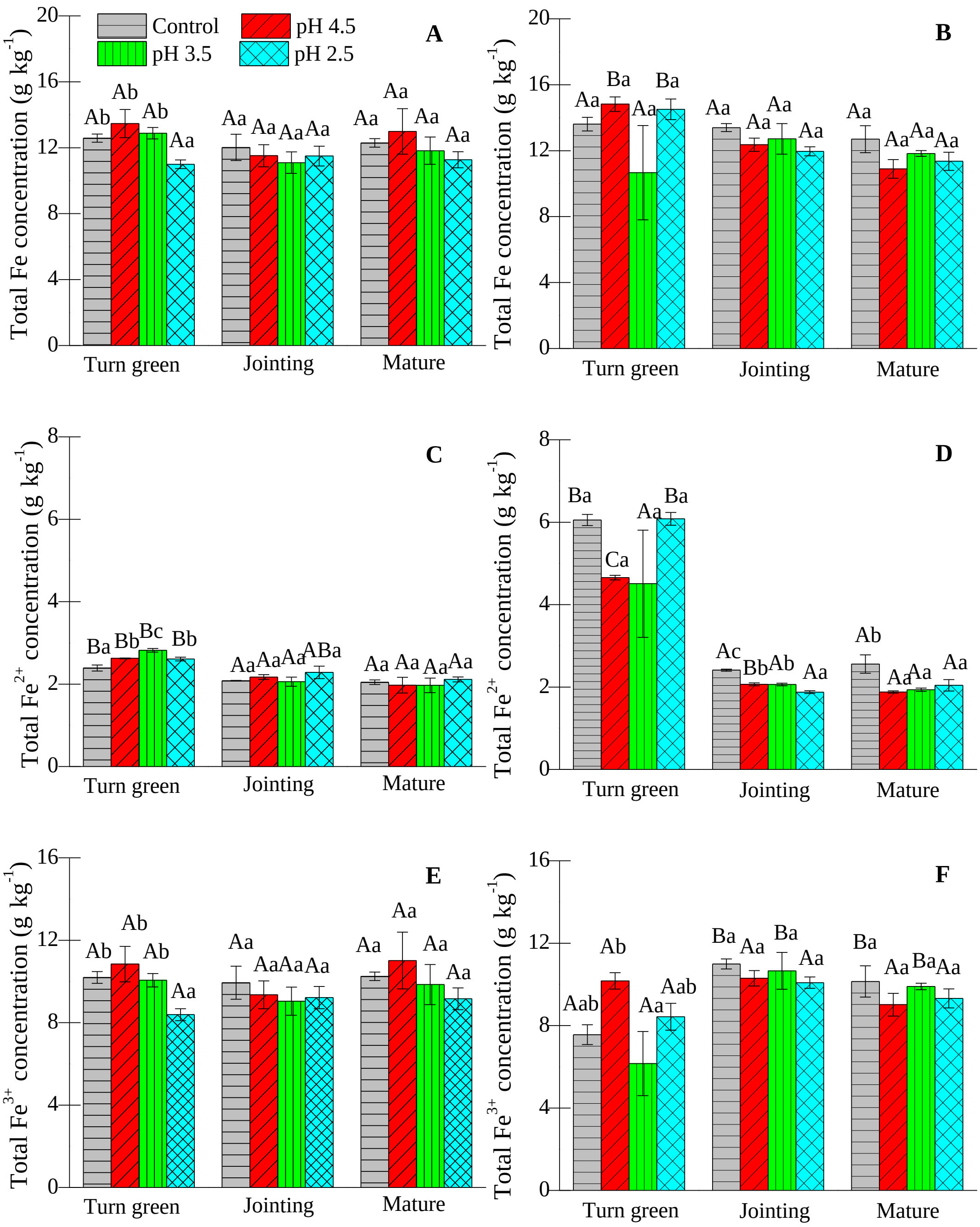
Control
pH 4.5
pH 3.5
pH 2.5
A
B
C
D
E
F
Total Fe concentration (g kg^{-1})
Total Fe^{2+} concentration (g kg^{-1})
Total Fe^{3+} concentration (g kg^{-1})
Turn green
Jointing
Mature

Fig. 5.

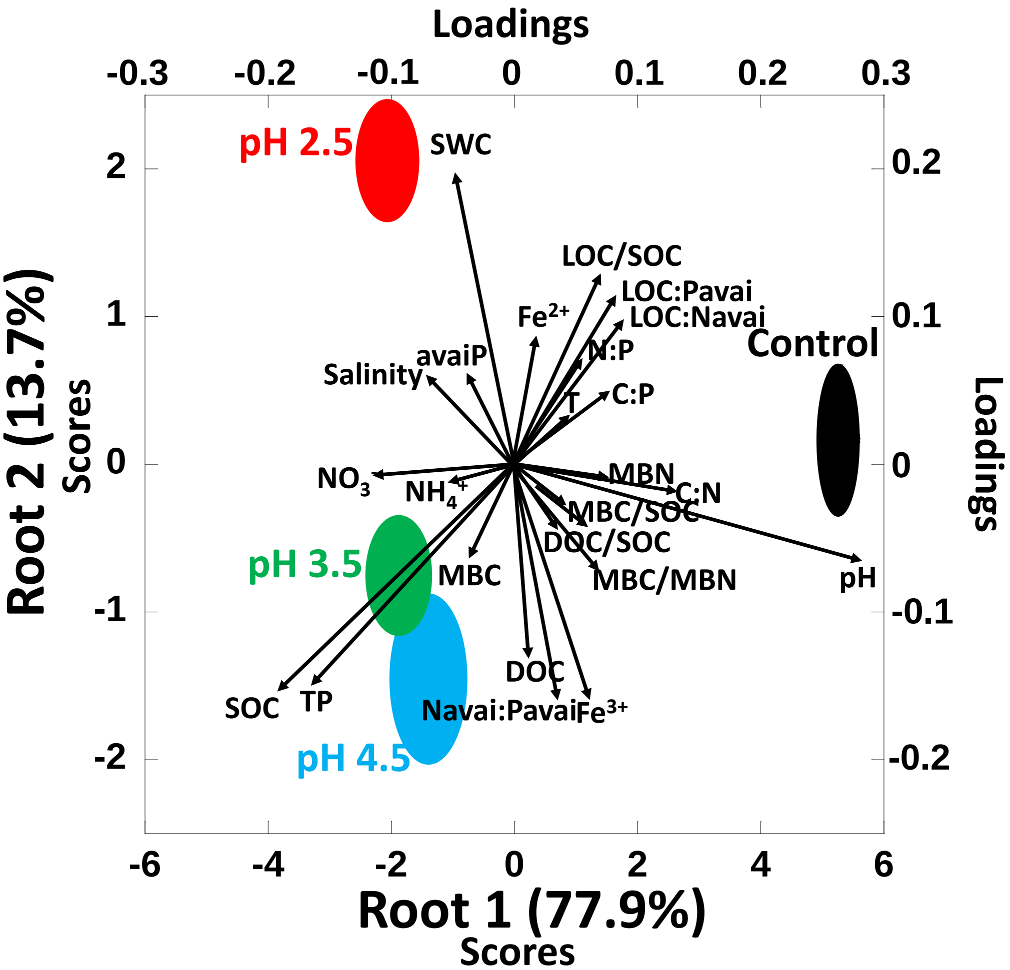
Loadings
-0.3
-0.2
-0.1
0
0.1
0.2
0.3
pH 2.5
SWC
LOC/SOC
LOC:Pavai
Fe2+
LOC:Navai
N:P
Control
Salinity
avaiP
T
C:P
NO3
NH4+
MBN
C:N
MBC/SOC
DOC/SOC
pH 3.5
MBC
MBC/MBN
pH
DOC
SOC
TP
Navai:Pavai
Fe3+
pH 4.5
Root 2 (13.7%)
Scores
2
1
0
-1
-2
0.2
0.1
0
-0.1
-0.2
Loadings
-6
-4
-2
0
2
4
6
Root 1 (77.9%)
Scores

Fig. 6.